

Heterogeneous Bond Percolation on Multitype Networks with an Application to Epidemic Dynamics

Antoine Allard, Pierre-André Noël, and Louis J. Dubé
*Département de physique, de génie physique et d'optique,
Université Laval, Québec, Québec, Canada G1V 0A6*

Babak Pourbohloul
*University of British Columbia Centre for Disease Control,
Vancouver, British Columbia, Canada V5Z 4R4 and
School of Population & Public Health, University of British Columbia, Vancouver, British Columbia, Canada V6T 1Z3*
(Dated: October 8, 2018)

Considerable attention has been paid, in recent years, to the use of networks in modeling complex real-world systems. Among the many dynamical processes involving networks, propagation processes — in which final state can be obtained by studying the underlying network percolation properties — have raised formidable interest. In this paper, we present a bond percolation model of multitype networks with an arbitrary joint degree distribution that allows heterogeneity in the edge occupation probability. As previously demonstrated, the multitype approach allows many non-trivial mixing patterns such as assortativity and clustering between nodes. We derive a number of useful statistical properties of multitype networks as well as a general phase transition criterion. We also demonstrate that a number of previous models based on probability generating functions are special cases of the proposed formalism. We further show that the multitype approach, by naturally allowing heterogeneity in the bond occupation probability, overcomes some of the correlation issues encountered by previous models. We illustrate this point in the context of contact network epidemiology.

PACS numbers: 89.75.Hc, 87.23.Ge, 05.70.Fh, 64.60.ah

I. INTRODUCTION

The end of the XXth century has witnessed increasing interest among the scientific community for the use of complex networks [1, 2, 3, 4] as models for many real-world systems, both from empirical and theoretical perspectives. From the empirical point of view, scientists have studied *real-world* networks to highlight universal topological properties such as the Small-World effect [5], highly skewed degree distributions [6, 7, 8, 9, 10] or assortative mixing [11]. On the theoretical side, models have been developed to describe or explain topological properties of networks [12, 13, 14, 15], to simulate their evolution in time [16] and the dynamical processes taking place on them [17, 18, 19, 20, 21].

The first models were rather simple: indistinguishable nodes joined by randomly placed edges [22]. With increasing information on real-world networks, more realistic — and thus more complex — models have been proposed taking into account properties such as an arbitrary degree distribution [13], clustering [23, 24], degree correlation [25], weighed edges [26, 27], directed edges [13, 28, 29, 30, 31, 32, 33] or mixing patterns [11, 34]. Except for a few cases (*e.g.* bipartite networks [13]), many existing models still consider only one type of nodes and therefore neglect any information characterizing the differences among the constituents of the simulated system. However, especially in social networks, these differences (*e.g.* sex, age, ethnic group) may have significant and non-trivial effects on the structure (*e.g.* assortative mix-

ing, communities) and on the dynamical property(ies) of the networks themselves as well as on the dynamics of the phenomena of interest (such as disease propagation) throughout the networks [35, 36].

In this paper, we present a bond percolation formalism of multitype networks with an arbitrary joint degree distribution where nodes have explicit properties associated with the type they belong to. On the one hand, the use of multitype networks allows one to reproduce mixing among nodes such as assortative mixing [25] or clustering [23]. On the other hand, the use of heterogeneous bond occupation probability allows one to take into account correlations between the probability of occupation of edges and the nature of the nodes they connect. When applied to epidemic propagation, we argue that this model adequately represents percolation (spreading) processes where such correlations are observed (*e.g.* infectious diseases whose probability of transmission is correlated with intrinsic physiological and behavioral characteristics of individuals).

Our paper is organized as follows. In Sec. II, we introduce the multitype networks and define several quantities of interest. The formalism is developed in Sec. III where we obtain the occupied degree (and excess degree) distributions, the small component sizes, the percolation threshold, and the giant and (average) small component sizes. We also show that our formalism corresponds to a generalization of existing approaches [19, 25, 37] reducing to known results in the appropriate limits. This theoretical section is validated with a number of numer-

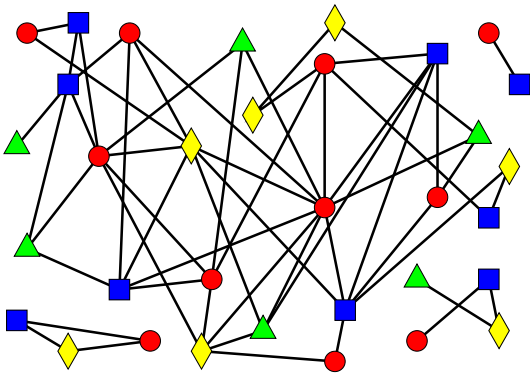


FIG. 1: (Color online) Schematic representation of an undirected *multitype* network with $M = 4$, $N = 33$, $w_1 = \frac{3}{11}$, $w_2 = \frac{1}{3}$, $w_3 = \frac{2}{11}$ and $w_4 = \frac{7}{33}$ where types 1,2,3 and 4 refer to squares, circles, triangles and diamonds respectively. Edges running between nodes are bidirectional and can thus be followed in either directions.

ical simulations and followed by an application to epidemic dynamics in Sec. IV, where the previously calculated quantities are interpreted in an epidemiological context. We also take the opportunity to explain how the proposed approach can overcome some of the correlation issues that should appear in a realistic treatment of epidemic propagation. Our conclusions and final remarks are then collected in the last section.

II. MULTITYPE NETWORKS

We consider undirected *multitype* networks [25, 38] defined as undirected networks composed of N nodes, each of which are labeled with one of M possible types. Type- i nodes occupy a fraction w_i of the network and the connections between nodes are prescribed by the degree distribution $P_i(k_1, k_2, \dots, k_M) \equiv P_i(\mathbf{k})$ giving the joint probability for a randomly chosen type- i node to be connected to k_1 type-1 nodes, k_2 type-2 nodes, \dots , k_M type- M nodes. Any mixing patterns between nodes such as assortative mixing are incorporated in the model via $P_i(\mathbf{k})$. Our networks are considered in the limit of large systems ($N \rightarrow \infty$) and are totally random in all respects other than the joint degree distribution $P_i(\mathbf{k})$ [54]. Therefore, $P_i(\mathbf{k})$ and w_i define a network ensemble over which all quantities obtained with our formalism are averaged. Fig. 1 shows an example of an undirected multitype network.

We now define z_{ij} as the average number of edges leaving a type- i node to type- j nodes, directly obtained from $P_i(\mathbf{k})$ as

$$z_{ij} = \sum_{k_1=0}^{\infty} \dots \sum_{k_M=0}^{\infty} k_j P_i(k_1, \dots, k_M) \equiv \sum_{\mathbf{k}=0}^{\infty} k_j P_i(\mathbf{k}). \quad (1)$$

Even if every edge in our networks is undirected, the presence of different types of nodes adds an *artificial* direc-

tion to edges. Indeed, one can follow a link from a type- i node to a type- j node (noted $i \rightarrow j$) or in the opposite direction ($j \rightarrow i$). Since the degree distribution $P_i(\mathbf{k})$ prescribes the number of edges *leaving* type- i nodes, a given edge joining a type- i and a type- j node will be considered from two different perspectives. Therefore, to guarantee the consistency of the network ensemble, $P_i(\mathbf{k})$ and w_i must respect the condition

$$\mathbf{wz} = (\mathbf{wz})^T \quad (2)$$

where

$$\mathbf{w} = \begin{bmatrix} w_1 & 0 & \dots & 0 \\ 0 & w_2 & \dots & 0 \\ \vdots & \vdots & \ddots & \vdots \\ 0 & 0 & \dots & w_M \end{bmatrix}; \quad \mathbf{z} = \begin{bmatrix} z_{11} & z_{12} & \dots & z_{1M} \\ z_{21} & z_{22} & \dots & z_{2M} \\ \vdots & \vdots & \ddots & \vdots \\ z_{M1} & z_{M2} & \dots & z_{MM} \end{bmatrix}$$

when $N \rightarrow \infty$. This constraint relies on having as many edges of type $i \rightarrow j$ as of type $j \rightarrow i$ [55]. Note that (2) implies $\binom{M}{2}$ non-trivial generally overdetermined equations. Thus, one must use values for $P_i(\mathbf{k})$ and w_i that explicitly fulfill (2). The case $M = 2$ is special in that w_i can be uniquely determined from $P_i(\mathbf{k})$

$$w_1 = \frac{z_{21}}{z_{12} + z_{21}}, \quad w_2 = \frac{z_{12}}{z_{12} + z_{21}}$$

with $\text{Tr}(\mathbf{w}) = 1$.

Having now defined networks where one can identify the type of nodes, we are able to apply different probabilities of occupation according to how edges are followed. Thus, instead of having only one edge occupation probability T , as in other percolation models [19], we define the bond occupation probability matrix

$$\mathbf{T} = \begin{bmatrix} T_{11} & T_{12} & \dots & T_{1M} \\ T_{21} & T_{22} & \dots & T_{2M} \\ \vdots & \vdots & \ddots & \vdots \\ T_{M1} & T_{M2} & \dots & T_{MM} \end{bmatrix} \quad (3)$$

where T_{ij} is the occupation probability of the $i \rightarrow j$ edges. Note that \mathbf{T} does not need to be symmetric and the probability of occupation of $i \rightarrow j$ edges can vary between edges of the same type (*i.e.* linking the same ordered pair ij) as long as those values are independent identically distributed (*iid*) random variables. The value of T_{ij} is then simply the mean of their distribution [19] and is totally independent of T_{ji} , which is the mean of a different and independent distribution.

In view of the possible asymmetry of the probability of occupation, our approach is somewhat different from the traditional bond percolation treatment which assumes a symmetric \mathbf{T} . It would perhaps be more appropriate to refer to our system as a *semi-directed bond percolation*. This denomination stems from the following point of view: one formally replaces every edge of the original undirected network by two directed edges running in opposite directions and then uses the corresponding probability of occupation for each directed edges. This leads

to a semi-directed network whose percolation properties are easier to analyse. Therefore, the introduction of multitypes together with the transmissibility matrix allows us to cover systems ranging from classical bond percolation (symmetric \mathbf{T}) to spreading processes (asymmetric symmetric \mathbf{T}) where directionality (e.g. causality) is implicitly present. On this basis, we develop the multitype formalism in the next section.

III. FORMALISM

We now present a formalism that describes the heterogeneous bond percolation of multitype networks. It is based on probability generating functions (PGF) [39] and is a generalization to multitype networks of the formalism developed earlier by Newman [19].

A. Occupied Degree Distribution

The first quantity needed to describe the percolation properties is the occupied degree distribution $\tilde{P}_i(\tilde{\mathbf{k}})$, *i.e.* the distribution of the number of occupied edges leaving a randomly chosen type- i node. Assuming independence in the edges' occupation state, the probability that a randomly chosen degree- \mathbf{k} node has $\tilde{\mathbf{k}}$ occupied edges is

$$P_i(\tilde{\mathbf{k}}|\mathbf{k}) = \prod_{l=1}^M \binom{k_l}{\tilde{k}_l} (T_{il})^{\tilde{k}_l} (1 - T_{il})^{k_l - \tilde{k}_l}. \quad (4)$$

The probability that a randomly chosen node has $\tilde{\mathbf{k}}$ occupied edges is then simply

$$\begin{aligned} \tilde{P}_i(\tilde{\mathbf{k}}) &= \sum_{\mathbf{k}=\tilde{\mathbf{k}}}^{\infty} P_i(\tilde{\mathbf{k}}|\mathbf{k}) P_i(\mathbf{k}) \\ &= \sum_{\mathbf{k}=\tilde{\mathbf{k}}}^{\infty} P_i(\mathbf{k}) \prod_{l=1}^M \binom{k_l}{\tilde{k}_l} (T_{il})^{\tilde{k}_l} (1 - T_{il})^{k_l - \tilde{k}_l}, \end{aligned} \quad (5)$$

where the summation convention is defined in (1) here covering the ranges $\tilde{k}_l \leq k_l \leq \infty$ for $1 \leq l \leq M$. This probability is generated by the PGF $G_i(\mathbf{x}; \mathbf{T}) \equiv G_i(x_1, \dots, x_M; \mathbf{T})$

$$\begin{aligned} G_i(\mathbf{x}; \mathbf{T}) &= \sum_{\tilde{\mathbf{k}}=\mathbf{0}}^{\infty} \tilde{P}_i(\tilde{\mathbf{k}}) \prod_{l=1}^M x_l^{\tilde{k}_l} \\ &= \sum_{\mathbf{k}=\mathbf{0}}^{\infty} P_i(\mathbf{k}) \prod_{l=1}^M \sum_{\tilde{k}_l=0}^{k_l} \binom{k_l}{\tilde{k}_l} (x_l T_{il})^{\tilde{k}_l} (1 - T_{il})^{k_l - \tilde{k}_l} \\ &= \sum_{\mathbf{k}=\mathbf{0}}^{\infty} P_i(\mathbf{k}) \prod_{l=1}^M [1 + (x_l - 1) T_{il}]^{k_l}. \end{aligned} \quad (6)$$

We see that $G_i(\mathbf{1}; \mathbf{T}) = 1$ if $P_i(\mathbf{k})$ is properly normalized. We can obtain the average occupied degree \tilde{z}_{ij} , *i.e.* the

average number of occupied edges leaving a type- i node to type- j nodes, by using the differentiation property [13] of generating functions

$$\begin{aligned} \tilde{z}_{ij} &= \frac{dG_i(\mathbf{1}; \mathbf{T})}{dx_j} \\ &= T_{ij} \sum_{\mathbf{k}=\mathbf{0}}^{\infty} k_j P_i(\mathbf{k}) \\ &= T_{ij} z_{ij} \end{aligned} \quad (7)$$

where z_{ij} is the average degree defined by (1).

B. Occupied *Excess* Degree Distribution

Another useful and accessible quantity in our formalism is the occupied *excess* degree distribution $\tilde{Q}_{ij}(\tilde{\mathbf{k}})$. The *excess* degree is defined as the number of edges leaving a node that have been reached by following a randomly chosen edge. For undirected *unitype* networks ($M = 1$), this quantity is simply the node's degree minus one (the edge that has already been followed). More information is required for multitype networks; one needs to know the type of node at both ends of the followed edge to correctly calculate the excess degree. This quantity is proportional to $k_i P_j(\mathbf{k})$ since high degree nodes are more likely to be reached from a randomly chosen edge than low degree nodes. Assuming independence in the occupation state of edges, the occupied excess degree distribution of a type- j node reached from an $i \rightarrow j$ edge is given by

$$\begin{aligned} \tilde{Q}_{ij}(\tilde{\mathbf{k}}) &= \frac{1}{z_{ji}} \sum_{\mathbf{k}=\tilde{\mathbf{k}}}^{\infty} (k_i + 1) P_j(\mathbf{k} + \boldsymbol{\delta}_i) \\ &\quad \times \prod_{l=1}^M \binom{k_l}{\tilde{k}_l} (T_{jl})^{\tilde{k}_l} (1 - T_{jl})^{k_l - \tilde{k}_l} \end{aligned} \quad (8)$$

where $P_j(\mathbf{k} + \boldsymbol{\delta}_i) \equiv P_j(k_1 + \delta_{i1}, \dots, k_M + \delta_{iM})$ and δ_{ij} is the delta of Krönercker. Defining $F_{ij}(\mathbf{x}; \mathbf{T})$ as the generating function associated with this distribution, we have

$$\begin{aligned} F_{ij}(\mathbf{x}; \mathbf{T}) &= \sum_{\tilde{\mathbf{k}}=\mathbf{0}}^{\infty} \tilde{Q}_{ij}(\tilde{\mathbf{k}}) \prod_{l=1}^M x_l^{\tilde{k}_l} \\ &= \frac{1}{z_{ji}} \sum_{\mathbf{k}=\mathbf{0}}^{\infty} k_i P_j(\mathbf{k}) \prod_{l=1}^M [1 + (x_l - 1) T_{jl}]^{k_l - \delta_{il}} \end{aligned}$$

which can also be obtained from $G_i(\mathbf{x}; \mathbf{T})$ by differentiation

$$F_{ij}(\mathbf{x}; \mathbf{T}) = \frac{1}{\tilde{z}_{ji}} \frac{dG_j(\mathbf{x}; \mathbf{T})}{dx_i} \quad (9)$$

where \tilde{z}_{ij} is the average occupied degree defined by (7).

obtain $\langle s_i \rangle$, one simply has to solve (14), M sets of M^2 equations and M^2 unknowns. It can be shown that all $\alpha_{ij}^{(i)}$ are inversely proportional to $\det(\mathbf{I} - \mathbf{A})$ where \mathbf{I} is the identity matrix and \mathbf{A} is a $M \times M$ block matrix whose blocks (\mathbf{A}_{ij}) are themselves $M \times M$ matrices with

$$[\mathbf{A}_{ij}]_{\mu\nu} = T_{ij} \beta_{\mu\nu}^{(j)} \delta_{i\nu} \quad (16)$$

giving the (μ, ν) element of the (i, j) block. For example, in the case $M = 2$, \mathbf{A} takes the form

$$\mathbf{A} = \begin{bmatrix} \begin{bmatrix} T_{11}\beta_{11}^{(1)} & 0 \\ T_{11}\beta_{21}^{(1)} & 0 \end{bmatrix} & \begin{bmatrix} T_{12}\beta_{11}^{(2)} & 0 \\ T_{12}\beta_{21}^{(2)} & 0 \end{bmatrix} \\ \begin{bmatrix} 0 & T_{21}\beta_{12}^{(1)} \\ 0 & T_{21}\beta_{22}^{(1)} \end{bmatrix} & \begin{bmatrix} 0 & T_{22}\beta_{12}^{(2)} \\ 0 & T_{22}\beta_{22}^{(2)} \end{bmatrix} \end{bmatrix}. \quad (17)$$

From (13), we see that the average size $\langle s \rangle$ of the component reached from a randomly chosen node diverges as

$$\langle s \rangle = \sum_{i=1}^M \langle s_i \rangle \propto \frac{1}{\det(\mathbf{I} - \mathbf{A})} \quad (18)$$

for $\det(\mathbf{I} - \mathbf{A}) \rightarrow 0$. Therefore the phase transition happens when $\det(\mathbf{I} - \mathbf{A}) = 0$ which marks the point where the giant component first appears. This result is in accord with the corresponding expression found in [25] and, as noted earlier, is again more general.

E. Giant Component

Beyond the percolation threshold, there is an *extensive* cluster (the giant component) in the network. In Sec. III C, $H_{ij}(\mathbf{x}; \mathbf{T})$ has been defined as generating the size distribution of *finite* components. Thus, $H_{ij}(\mathbf{x}; \mathbf{T})$, $K_i(\mathbf{x}; \mathbf{T})$ and $K(\mathbf{x}; \mathbf{T})$ are no longer normalized beyond the percolation threshold since it is not guaranteed that a randomly chosen edge/node will lead to a finite component (although a fraction of them may lead to the giant component). Therefore, the probability that a randomly chosen type- i node leads to the giant component is simply

$$\begin{aligned} \mathcal{P}_i &= 1 - K_i(\mathbf{1}; \mathbf{T}) \\ &= 1 - G_i(\vec{\mathbf{h}}_i; \mathbf{T}) \end{aligned} \quad (19)$$

with $G_i(\vec{\mathbf{h}}_i; \mathbf{T}) \equiv G_i(\vec{h}_{i1}, \dots, \vec{h}_{iM}; \mathbf{T})$. We have noted $\vec{h}_{ij} \equiv H_{ij}(\mathbf{1}; \mathbf{T})$ (read h_{ij} *forward*) as the probability that a randomly chosen $i \rightarrow j$ edge leads to a finite component, and is the solution of

$$\vec{h}_{ij} = F_{ij}(\vec{\mathbf{h}}_j; \mathbf{T}) \quad (20)$$

obtained by evaluating (10) at $\mathbf{x} = \mathbf{1}$. If one randomly chooses a node in the network, the probability that it leads to the giant component is therefore

$$\mathcal{P} = \sum_{i=1}^M w_i \mathcal{P}_i = 1 - \sum_{i=1}^M w_i G_i(\vec{\mathbf{h}}_i; \mathbf{T}). \quad (21)$$

To calculate the size of the giant component, one needs to know the probability that a randomly chosen node is *not* linked to the giant component by any of its edges (*i.e.* that this node can not be reached from the giant component). One simple way to obtain this information is to study the network topology by following every edges *backwards*. This can be achieved with our formalism by simply using \mathbf{T}^T (the transpose of \mathbf{T}) instead of \mathbf{T} since any given type- i node can be left (reached) by any of its edges with the probability T_{ij} (T_{ji}). We define \overleftarrow{h}_{ij} (read h_{ij} *backward*) as the probability that a given type- i node can not be reached from the giant component by a $j \rightarrow i$ edge. This quantity is calculated as solution of

$$\overleftarrow{h}_{ij} = F_{ij}(\overleftarrow{\mathbf{h}}_j; \mathbf{T}^T). \quad (22)$$

Therefore, we see that $G_i(\overleftarrow{\mathbf{h}}_i; \mathbf{T}^T)$ is the probability that a randomly chosen type- i node does not belong to the giant component. The fraction of the network occupied by type- i nodes that are in the giant component is thus given by

$$\mathcal{S}_i = w_i [1 - G_i(\overleftarrow{\mathbf{h}}_i; \mathbf{T}^T)] \quad (23)$$

and the size of the giant component is

$$\mathcal{S} = \sum_{i=1}^M \mathcal{S}_i = 1 - \sum_{i=1}^M w_i G_i(\overleftarrow{\mathbf{h}}_i; \mathbf{T}^T). \quad (24)$$

In comparing (21) and (24), one will see that asymmetry of the bond occupation probability matrix implies that $\mathcal{P} \neq \mathcal{S}$. This quantitative difference between \mathcal{P} and \mathcal{S} resides in the asymmetry in the number of occupied edges of type $i \rightarrow j$ and of type $j \rightarrow i$. A naive generalization of the formalism introduced in [19] would have missed the distinction between \mathcal{P} and \mathcal{S} . Clearly for symmetric transmissibility $\mathbf{T} = \mathbf{T}^T$, one would have $\mathcal{P} = \mathcal{S}$. A similar result has previously been discussed in [31] for semi-directed networks and, with different approaches, it has been obtained for *undirected* networks in [36, 51]. The present demonstration is a new extension to the latter class of networks.

F. Average Small Components Size

Above the percolation threshold, $K(\mathbf{x}; \mathbf{T})$ still generates the size distribution of the finite component reached from a randomly chosen node, although it needs to be normalized according to

$$\frac{K(\mathbf{x}; \mathbf{T})}{1 - \mathcal{P}}$$

since $\mathcal{P} \neq 0$. The general expression for $\langle s_i \rangle$ is therefore

$$\langle s_i \rangle = \frac{w_i G_i(\vec{\mathbf{h}}_i; \mathbf{T})}{1 - \mathcal{P}} + \frac{1}{1 - \mathcal{P}} \sum_{l=1}^M w_l \sum_{j=1}^M \tilde{z}_{lj} \vec{h}_{jl} \alpha_{ij}^{(i)} \quad (25)$$

where $\alpha_{lj}^{(i)}$ is the average number of type- i nodes in the finite component reached by a randomly chosen $l \rightarrow j$ edge and is the solution of

$$\alpha_{lj}^{(i)} = F_{lj}(\vec{h}_j; \mathbf{T})\delta_{ij} + \sum_{n=1}^M T_{jn}\beta_{lj}^{(n)}\alpha_{jn}^{(i)}. \quad (26)$$

Analogously to (15),

$$\beta_{lj}^{(n)} = \frac{1}{T_{jn}} \left. \frac{\partial F_{lj}(\mathbf{x}; \mathbf{T})}{\partial x_n} \right|_{\mathbf{x}=\vec{h}_j}. \quad (27)$$

One can see that (25)–(27) reduce to (13)–(15) in absence of the giant component since in this case $\mathcal{P} = 0$ and $\vec{h}_{ij} = 1$. Technically, (25)–(27) can be very useful to obtain information on the small components without having to solve (10)–(12), a very time consuming operation for large M or for networks with large small components. It is also possible to calculate the second moments of $K(\mathbf{x}; \mathbf{T})$

$$\langle s_i s_j \rangle = \frac{1}{1 - \mathcal{P}} \frac{d}{dx_j} \left[x_i \frac{dK(\mathbf{x}; \mathbf{T})}{dx_i} \right] \Bigg|_{\mathbf{x}=1} \quad (28)$$

from which the covariance matrix of the small components size ($\text{cov}\{s_i, s_j\} = \langle s_i s_j \rangle - \langle s_i \rangle \langle s_j \rangle$) is obtained. Clearly, iterative equations for $\langle s_i s_j \rangle$, similar to (25) and (26), can be derived to calculate the covariance matrix without solving (10)–(12). Higher moments can also be obtained in a similar way.

G. Special Cases

We now show that, in corresponding limit cases, our formalism reproduces the already published theoretical results. Firstly, one can easily verify that all of the equations in the previous section reduce to the ones in [19] when $M = 1$. Secondly, equations associated with the components (small or giant) in [25] can be obtained by setting $T_{ij} = 1 \forall i, j$ in our equations and $\mathbf{x} = x$ in (10) and (11). Thirdly, results obtained from a semi-directed formalism such as the one in [31] can also be obtained with our formalism by setting $T_{ij} = 0$ for some ij pairs while keeping $T_{ji} \neq 0$. Fourthly, for bipartite networks ($M = 2$), all edges are connecting different types of nodes and the constraint

$$P_i(k_1, k_2) = 0 \forall k_i \neq 0$$

must be imposed, implying that

$$z_{ii} = 0; \quad \beta_{ii}^{(j)} = 0; \quad \beta_{ji}^{(i)} = 0; \quad \alpha_{ii}^{(j)} = 0.$$

$F_{ii}(x_1, x_2; \mathbf{T})$ and $H_{ii}(x_1, x_2; \mathbf{T})$ are then undefined. From (16), we see that the phase transition in this case, $\det(\mathbf{I} - \mathbf{A}) = 0$, occurs when

$$T_{12}T_{21}\beta_{12}^{(1)}\beta_{21}^{(2)} = 1,$$

a result previously obtained in [19, 37]. Moreover, one can obtain the average number of type-1 nodes in the component reached from a randomly chosen type-1 node $\langle s_1 \rangle_1$ under the percolation threshold by differentiating (11) with respect to x_i and solving (26)

$$\langle s_1 \rangle_1 = 1 + \frac{T_{12}T_{21}z_{12}\beta_{12}^{(1)}}{1 - T_{12}T_{21}\beta_{12}^{(1)}\beta_{21}^{(2)}},$$

a result also obtained by the authors of [19, 37]. Furthermore, it is possible to calculate the size of the giant component as in [37] by setting $x_2 = 1$ in (10) and (11) with the constraints listed above.

An even more general constraint $P_i(\mathbf{k}) = 0 \forall k_i \neq 0$ can be used to obtain a formalism for multipartite networks. Our approach can therefore incorporate clustering effects by assigning some of the node types to groups and then using the projected network (where nodes belonging to the same group are linked together) as proposed in [23].

IV. APPLICATION TO EPIDEMIOLOGY

Over the years, mathematical models [41, 42] have provided insights on the factors influencing diseases propagation dynamics and have improved testing intervention/prevention strategies. Outbreaks of respiratory pathogens (*e.g.* SARS [43]) and sexually transmitted infections (STIs) have encouraged the emergence of models using network theory to capture the patterns of potential disease-causing interactions between individuals [19, 20, 31, 44]. Despite the many successes, most of these models are still based on a simplifying assumption, which limits the realistic simulation of disease propagation for certain categories of diseases. Before discussing how the quantities obtained from our formalism can be translated in an epidemiological setting, we briefly state some of the difficulties associated with a realistic epidemic dynamics and the possible advantage of a multitype description.

A. Failure of the *iid* hypothesis and heterogeneity

The *iid* hypothesis [19] assumes that the probability of transmission between any pair of individuals is an *independent identically distributed* random variable taken from a given distribution. Thus, the *a priori* probability of transmission, T , between any two individuals is the mean of this distribution and, in the population as a whole, the disease will propagate from an infectious individual to a susceptible one with the same probability T . This implies that no correlations, whatsoever, can be taken into account.

However, the probability of transmission of infectious diseases is typically dependent on intrinsic immunological and behavioral traits of individuals. Many infectious diseases show heterogeneity in their transmissibility. For

example, the human immunodeficiency virus (HIV) has a higher efficiency of transmission from male to female than female to male [45, 46]. There is also strong evidence that co-infection with other STIs could facilitate HIV transmission [47, 48, 49]. In regards to influenza, it has been shown that children (under 15 years old) are more likely to transmit the disease than adults [50]. Further, it has been shown that the *iid* hypothesis fails to adequately model *susceptible-infectious-recovered* (SIR) dynamics when the distribution of the infectious period $P(\tau)$ is not sharp around a given value τ_0 [51, 52]. Therefore, most existing percolation approaches fail to realistically simulate the propagation of some infectious diseases due to the inability of the *iid* hypothesis to model the correlations between individual's traits (including their infectious period) and the probability of transmission.

If one could identify specific individuals within the network, one could determine *who infects whom* and it would become possible to apply the appropriate probability of transmission. Hence, difficulties raised by the heterogeneity in transmissibility could be largely overcome by considering node heterogeneity. This suggests that, in order to properly model the propagation of a large class of diseases, one could separate the nodes into a sufficient number of categories (types) to insure that the *iid* hypothesis can be applied correctly. Our multitype formalism can then be used to investigate the percolation properties of the corresponding system.

Confronted with a situation where the infectious period is broadly distributed and heterogeneity is present, one could adopt the following line of action. In the case of influenza, one could split the population between adults and children; or between male and female when modeling HIV propagation. The probability of transmission could still vary according to the *iid* hypothesis, within the same type of edges, if nodes are separated into a sufficient number of groups, within each of which all significant correlations are explicitly included. The finite width of the infectious period distribution $P(\tau)$ can be accounted for by simply dividing its contribution into a sufficient number of duration subdomains $[\tau_{i-1}, \tau_i]$ (each associated with a node type randomly distributed in the population if more detailed information is not available) and using the corresponding transmissibility in our model. The fraction of the network occupied by type- i nodes will then be $w_i = \int_{\tau_{i-1}}^{\tau_i} P(\tau) d\tau$. The same procedure is also applicable if the susceptibility of individuals is heterogeneous.

B. Epidemiological quantities

We now interpret the quantities that can be calculated with our formalism in an epidemiological context. The contact network topology is prescribed by $P_i(\mathbf{k})$ and w_i while the bond occupation probability matrix entries, T_{ij} , are the average probability of transmission from infectious individuals of type i to susceptible individuals of type j . $K_i(\mathbf{x}; \mathbf{T})$ generates the outbreak size distribution

caused by patient zero (*i.e.* the first known individual to become infected who directly or indirectly causes all subsequent infections) of type- i (*e.g.* adult, child; male, female). Similarly, $K(\mathbf{x}; \mathbf{T})$ generates the outbreak size distribution caused by a patient zero of any type. The quantity $\langle s_i \rangle$ is the average number of type- i individuals infected from patient zero and $\langle s \rangle = \sum_{i=1}^M \langle s_i \rangle$ is the expected size of an outbreak. One could also differentiate (11) with respect to x_j to obtain the average number of type- j individuals infected by a patient zero of type- i (see Sec. III G). Those quantities can be useful, for example, in evaluating the impact of strategies focused on the reduction of morbidity in specific population groups (*e.g.* health care workers, the elderly).

For a given contact network, $\det(\mathbf{I} - \mathbf{A})$ is a polynomial in powers of the elements of \mathbf{T} whose coefficients depend only of the network topology. Thus, the percolation threshold, $\det(\mathbf{I} - \mathbf{A}) = 0$, defines the *critical transmissibility set* over which there is a non-zero probability that an outbreak will turn into a large-scale epidemic. The probability that such an epidemic will occur is given by \mathcal{P} and by \mathcal{P}_i if patient zero is known to be of type- i . Should an epidemic occur, the fraction of the population that will eventually be infected is given by \mathcal{S} while \mathcal{S}_i indicates the fraction of the population of infected individuals of type i . Note that if an outbreak dies out while having infected only a finite number of individuals (or a small number compared to the size of the population), the expected number of infected individuals of type i is still given by $\langle s_i \rangle$ computed with (25) (this remark holds for $\langle s \rangle$ as well).

C. Numerical Simulations

To illustrate how our formalism could be applied in an epidemiological context and to confirm its predictions, we have performed extensive computer simulations on multitype networks of $N = 10^5$ nodes divided into two types ($M = 2$). We have considered a contact network where the distribution of the total degree ($k_1 + k_2$) of individuals is given by a power-law with an exponential cutoff and where the probability that an edge leaving a type- i node arrives on a type- j node is given by p_{ij} . Thus, the joint degree distribution of our network is

$$P_i(k_1, k_2) = \frac{(k_1 + k_2)^{-\eta_i} e^{-(k_1 + k_2)/\kappa_i}}{\text{Li}_{\eta_i}(e^{-1/\kappa_i})} \cdot \binom{k_1 + k_2}{k_1} p_{i1}^{k_1} p_{i2}^{k_2}$$

with the parameters

$$\boldsymbol{\eta} = \begin{bmatrix} 1 \\ 2 \end{bmatrix}; \quad \boldsymbol{\kappa} = \begin{bmatrix} 8 \\ 10 \end{bmatrix}; \quad \mathbf{p} = \begin{bmatrix} 0.7 & 0.3 \\ 0.4 & 0.6 \end{bmatrix}.$$

$\text{Li}_{\eta}(z)$ denotes the η th polylogarithm of z [53] (also known as Jonquière's function). We have used a simple joint degree distribution to illustrate our point; nonetheless our formalism is very general and $P_i(\mathbf{k})$ could include many non-trivial correlations as shown in [25]. To show

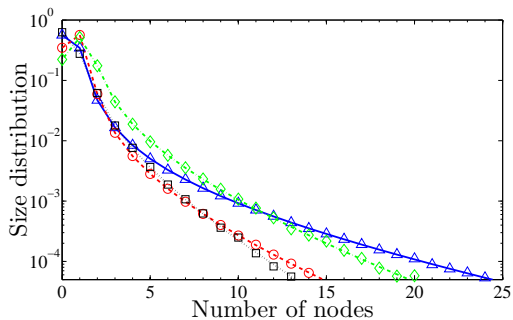


FIG. 3: (Color online) Size distribution of small components obtained by numerical simulations (symbols) compared with the theoretical prediction of (12) (lines). \triangle and \diamond correspond to the number of type-1 nodes in small components (generated by $K(x_1, 1; \mathbf{T})$) for $\gamma = 0.1$ and $\gamma = 0.5$ respectively. \circ and \square are the equivalent quantities but for type-2 nodes (generated by $K(1, x_2; \mathbf{T})$).

the effect of the asymmetry of \mathbf{T} on \mathcal{P} and \mathcal{S} , we have used the following transmissibility matrix

$$\mathbf{T} = \gamma \begin{bmatrix} 0.95 & 0.98 \\ 0.48 & 1.00 \end{bmatrix}$$

where γ allows us to vary the infectiousness of the disease. The specific choice of the elements of \mathbf{T} has no particular relevance here, except perhaps to result in large \mathcal{P} and \mathcal{S} values for $\gamma = 1$. By solving $\det(\mathbf{I} - \mathbf{A}) = 0$ for γ , we find that the epidemic transition occurs when $\gamma_c \simeq 0.1834$.

We have generated 2000 multitype networks following a method similar to the one described in [25], with the degree distribution presented above. We have then performed epidemic simulations by infecting a randomly chosen node and allowing the disease to propagate with probabilities given by \mathbf{T} . Above the percolation threshold, we have identified the components (small or giant) by setting a size-parameter, a percentage of the total number of nodes, below which the cluster was registered to belong to the set of small components. Experimentation has shown the final results rather insensitive to the exact value of the size-parameter and we have settled conservatively for a value of 0.5% of N . Figure 3 compares the distribution of the number of infected nodes of each type caused by an outbreak predicted by (12), with the results of numerical simulations under ($\gamma = 0.1$) and above ($\gamma = 0.5$) the epidemic threshold. One observes a very good agreement between the theoretical prediction and the simulations. This quantitative accord (in this figure and the following ones) is representative of a much larger set of calculations carried out with different values of the transmissibility matrix elements. Figure 4 shows the average number of infected nodes in an outbreak for each type of node and for different values of γ . Theoretical predictions are obtained from (25). Again, an excellent agreement between our model predictions and numerical simulations is recorded; the small disagreement around

the percolation threshold is caused by the finite size of the networks used for the simulations. Indeed as N decreases, finite size effects become important and the formalism would have to be modified along the lines described in [52], for instance. Preliminary results indicate however that agreement between results of the present formalism and numerical simulations is maintained, even if the size of the network is reduced to $N = 1000$. A more extensive study of the issue of finite size in a multitype network is under investigation.

Finally, Fig. 5 compares the values predicted by our model for the probability of an epidemic to occur (\mathcal{P}) and its relative size (\mathcal{S}_1 , \mathcal{S}_2 and \mathcal{S}) with simulation results for different values of γ . Again, there is a very good agreement between the theoretical predictions and results from simulations. The asymmetry of \mathbf{T} is responsible for the significant difference between \mathcal{P} and \mathcal{S} (up to approximately 10% in this case). We also see that the presence of node types allows more detailed information on the final state of an epidemic since it is then possible to determine the number of individuals of each type that are infected during an epidemic. Moreover, Fig. 5 demonstrates that these numbers do not remain proportional for varying transmissibilities. To the best of our knowledge, such information was not possible to obtain in previous percolation models. Furthermore, the heterogeneity in transmissibility in our formalism allows one to test more specific public-health policies. For instance, one could study the effectiveness of age-specific influenza control strategies such as vaccination, face masks or hand-washing by varying the transmissibility matrix entries for the relevant age groups. Therefore, the multitype approach of our model offers more detailed information on outbreak outcomes. This is very useful when comparing the cost-effectiveness of prevention or intervention strategies.

V. CONCLUSION

In this paper, we have introduced a bond percolation formalism on multitype networks. The formalism explicitly allows heterogeneity in the edge occupation probability via the matrix \mathbf{T} whose elements T_{ij} are the probability for an $i \rightarrow j$ edge to be occupied. Using probability generating functions (PGF), we have obtained several exact forms of classical statistical properties (in the limit of large networks) such as, the size distribution of small components, the probability of reaching the giant component from any node as well as its relative size. Furthermore, the presence of node types has allowed us to obtain more detailed information on the composition of small components, the giant component, and a general expression for the percolation threshold. We have also obtained iterative equations for the average number of type- i nodes in the small component, which allows to easily and rapidly obtain information on the network structure.

We have also shown that our model is a generalized

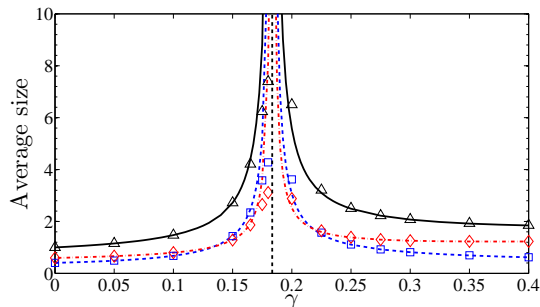


FIG. 4: (Color online) Average number of nodes in small components as predicted by (25) (lines) compared to simulations results (symbols; \square : type-1 nodes, \diamond : type-2 nodes and \triangle : both) as a function of γ . The vertical dashed black line indicates the percolation threshold (γ_c).

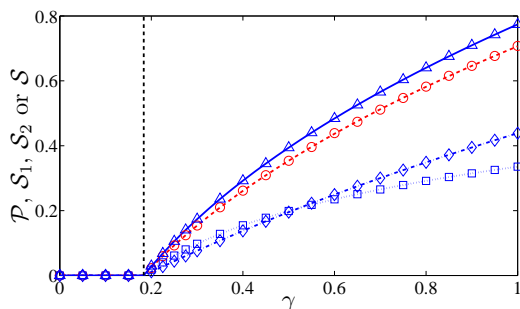


FIG. 5: (Color online) Probability of reaching the giant component from a randomly chosen node (\mathcal{P} , \circ), fraction of the network occupied by type-1 nodes (\mathcal{S}_1 , \square), type-2 nodes (\mathcal{S}_2 , \diamond) and both node types (\mathcal{S} , \triangle) in the giant component. Lines stand for theoretical predictions and symbols for simulation results. The vertical dashed black line indicates the percolation threshold (γ_c).

version of various existing approaches based on the PGF. Many known results and effects can be obtained with our model. For instance, equations describing the bond percolation of multipartite networks can easily be derived from our formalism. While semi-directed networks have been previously used to simulate the asymmetry between population groups infecting each other [31], this effect can be achieved with our undirected network model by setting $T_{ij} = 0$ for some ij pairs while keeping $T_{ji} \neq 0$. Thus, type- j nodes will be able to infect type- i nodes, while transmission in the other direction will not be possible. A completely general semi-directed extension of

our formalism (with $3M$ variables, say \mathbf{x} , \mathbf{y} , \mathbf{z} , for the 3 ways to move across the network, following the links forward, backward and in both directions) is straightforward to derive. This extended formalism would be required when the underlying network includes directed edges whose presence can not be randomly determined with a probability T_{ij} that solely depends on the edge type (here $i \rightarrow j$), *i.e.*, additional correlations exist.

These structural properties have considerable influence on the dynamical processes taking place on networks; this, in turn, can have a significant impact on their topology. Therefore, a formalism such as the one presented in this paper can be used to probe and characterize the structure (by setting $T_{ij} = 1 \forall i, j = 1, \dots, M$) of an evolving network at a given time in order to predict the network's topological evolution.

The approach described in this paper, when compared to previous methods, facilitates more realistic simulations of the propagation of infectious diseases manifesting heterogeneity in their transmissibility. We argue that heterogeneity in nodes is a way to overcome some correlation issues caused by heterogeneous transmissibility. In addition, the presence of different types of nodes allows the simulation of many non-trivial mixing patterns observed in real-world networks, such as assortativity, the preferential connection between different types of nodes; and clustering, the fact that nodes belonging to a specific group are more likely to be connected to one another in the contact network. Thus, the proposed model is suitable for more detailed and more precise epidemiological investigations (*e.g.* impact of intervention or prevention strategies on specific population groups) resulting in more adapted and effective recommendations to public health authorities. Hopefully, models such as the one presented in this paper joined with ever increasing theoretical developments will contribute to the improvement of public health policies.

Acknowledgments

BP acknowledges the support of the Canadian Institutes of Health Research (CIHR, grants no. MOP-81273 and PPR-79231), the Michael Smith Foundation for Health Research (Senior Scholar Funds) and the British Columbia Ministry of Health (Pandemic Preparedness Modeling Project). AA and PAN were partly supported by the above grants and PAN is also thankful to CIHR for further support. LJD is grateful to NSERC (Canada) and FQRNT (Québec) for continuing support.

-
- [1] R. Albert and A.-L. Barabási, *Rev. Mod. Phys.* **74**, 47 (2002).
 [2] S. Boccaletti, V. Latora, Y. Moreno, M. Chavez, and D.-U. Hwang, *Phys. Rep.* **424**, 175 (2006).

- [3] S. N. Dorogovtsev and J. F. F. Mendes, *Advances in Physics* **51**, 1079 (2002).
 [4] M. E. J. Newman, *SIAM Review* **45**, 167 (2003).
 [5] D. J. Watts and S. H. Strogatz, *Nature* **393**, 440 (1998).

- [6] R. Albert, H. Jeong, and A.-L. Barabási, *Nature* **401**, 130 (1999).
- [7] H. Jeong, B. Tombor, R. Albert, Z. N. Oltvai, and A.-L. Barabasi, *Nature* **407**, 651 (2000).
- [8] F. Liljeros, C. R. Edling, L. A. N. Amaral, H. E. Stanley, and Y. Aberg, *Nature* **411**, 907 (2001).
- [9] S. Redner, *Eur. Phys. J. B* **4**, 131 (1998).
- [10] A. Vazquez, R. Pastor-Satorras, and A. Vespignani, *Phys. Rev. E* **65**, 066130 (2002).
- [11] M. E. J. Newman, *Phys. Rev. Lett.* **89**, 208701 (2002).
- [12] A.-L. Barabási and R. Albert, *Science* **286**, 509 (1999).
- [13] M. E. J. Newman, S. H. Strogatz, and D. J. Watts, *Phys. Rev. E* **64**, 026118 (2001).
- [14] J. Park and M. E. J. Newman, *Phys. Rev. E* **70**, 066117 (2004).
- [15] R. Pastor-Satorras and A. Vespignani, *Evolution and Structure of the Internet: A Statistical Physics Approach* (Cambridge University Press, Cambridge, 2004).
- [16] T. Gross and B. Blasius, *J. R. Soc. Interface* **5**, 259 (2008).
- [17] R. Albert, H. Jeong, and A.-L. Barabási, *Nature* **406**, 378 (2000).
- [18] Y. Moreno, M. Nekovee, and A. F. Pacheco, *Phys. Rev. E* **69**, 066130 (2004).
- [19] M. E. J. Newman, *Phys. Rev. E* **66**, 016128 (2002).
- [20] R. Pastor-Satorras and A. Vespignani, *Phys. Rev. Lett.* **86**, 3200 (2001).
- [21] H. P. Young, in *The Economy as an Evolving Complex System, Vol. 3*, edited by L. E. Blume and S. N. Durlauf (Oxford University Press, Oxford, 2003).
- [22] P. Erdős and A. Rényi, *Publ. Math. Debrecen* **6**, 290 (1959).
- [23] M. E. J. Newman, *Phys. Rev. E* **68**, 026121 (2003).
- [24] M. A. Serrano and M. Boguñá, *Phys. Rev. Lett.* **97**, 088701 (2006).
- [25] M. E. J. Newman, *Phys. Rev. E* **67**, 026126 (2003).
- [26] M. E. J. Newman, *Phys. Rev. E* **70**, 056131 (2004).
- [27] S. H. Yook, H. Jeong, A.-L. Barabási, and Y. Tu, *Phys. Rev. Lett.* **86**, 5835 (2001).
- [28] G. Bianconi, N. Gulbahce, and A. E. Motter, *Phys. Rev. Lett.* **100**, 118701 (2008).
- [29] M. Boguñá and M. A. Serrano, *Phys. Rev. E* **72**, 016106 (2005).
- [30] E. A. Leicht and M. E. J. Newman, *Phys. Rev. Lett.* **100**, 118703 (2008).
- [31] L. A. Meyers, M. E. J. Newman, and B. Pourbohloul, *J. Theor. Biol.* **240**, 400 (2006).
- [32] J. G. Restrepo, E. Ott, and B. R. Hunt, *Phys. Rev. Lett.* **100**, 058701 (2008).
- [33] N. Schwartz, R. Cohen, D. ben-Avraham, A.-L. Barabási, and S. Havlin, *Phys. Rev. E* **66**, 015104(R) (2002).
- [34] M. Catanzaro, G. Caldarelli, and L. Pietronero, *Physica A* **338**, 119 (2004).
- [35] T. Gross, Carlos J. Dommar DLima, and B. Blasius, *Phys. Rev. Lett.* **96**, 208701 (2006).
- [36] J. C. Miller, *Phys. Rev. E* **76**, 010101(R) (2007).
- [37] L. A. Meyers, M. E. J. Newman, M. Martin, and S. Schrag, *Emerg. Infect. Dis.* **9**, 204 (2003).
- [38] A. Vazquez, *Phys. Rev. E* **74**, 066114 (2006).
- [39] H. S. Wilf, *generatingfunctionology* (Academic Press inc., 1994), 2nd ed.
- [40] D. Stauffer and A. Aharony, *Introduction to Percolation Theory* (Taylor & Francis, 1994), revised second ed.
- [41] R. M. Anderson and R. M. May, *Infectious Diseases of Humans: Dynamics and Control* (Oxford University Press, Oxford, 1991).
- [42] H. S. Hethcote, *SIAM Review* **42**, 599 (2000).
- [43] L. A. Meyers, B. Pourbohloul, M. E. J. Newman, D. M. Skowronski, and R. C. Brunham, *J. Theor. Biol.* **232**, 71 (2005).
- [44] Y. Moreno, R. Pastor-Satorras, and A. Vespignani, *Eur. Phys. J. B* **26**, 521 (2002).
- [45] A. Nicolosi, M. C. Leite, M. Musicco, C. Arici, G. Gavazzeni, and A. Lazzarin, *Epidemiology* **5**, 570 (1994).
- [46] J. R. Glynn, M. Carael, B. Auvert, M. Kahindo, J. Chege, R. Musonda, F. Kaona, A. Buve, and the Study Group on the Heterogeneity of HIV Epidemics in African Cities, *AIDS* **15** (suppl. 4), S51 (2001).
- [47] P. L. Vernazza, J. J. Eron, S. A. Fiscus, and M. S. Cohen, *AIDS* **13**(2), 155 (1999).
- [48] H. Grosskurth, F. Mosha, J. Todd, K. Senkoro, J. Newell, A. Klokke, J. Changalucha, B. West, P. Mayaud, A. Gavyole, et al., *AIDS* **9**, 927 (1995).
- [49] J. N. Wasserheit, *Sex. Transm. Dis.* **19**, 61 (1992).
- [50] S. Cauchemez, F. Carrat, C. Viboud, A. J. Valleron, and P. Y. Boëlle, *Statist. Med.* **23**, 3469 (2004).
- [51] E. Kenah and J. M. Robins, *Phys. Rev. E* **76**, 036113 (2007).
- [52] P.-A. Noël, B. Davoudi, R. C. Brunham, L. J. Dubé, and B. Pourbohloul, accepted for publication Dec. 2008, *Phys. Rev. E*79, e-print arXiv:0804.1807v4 [q-bio.PE] (2008).
- [53] L. Lewin, *Polylogarithms and Associated Functions* (Elsevier North Holland, New York, 1981).
- [54] We consider *simple* networks where no more than one edge can exist between two nodes and where there is no edge connecting a node to itself. The two possibilities have a probability of the order of $\mathcal{O}(N^{-2})$ and $\mathcal{O}(N^{-1})$ respectively in large random networks of size N .
- [55] In practice, for realistic data, there will be as many edges of type $i \rightarrow j$ as of type $j \rightarrow i$ and (2) will naturally be respected.
- [56] In an *infinite* network, $H_{ij}(\mathbf{x}; \mathbf{T})$ is invariant under translation on the network, *i.e.* one always sees the same small components size distribution independently where he/she stands in the small component.